sustainability

MDPI

Article

Reaction Behavior and Transformation Path of Zinc in the Heating-Up Zone during Sintering Process

Wei Lv [1,2], Min Gan [1,*], Xiaohui Fan [1,*], Zengqing Sun [1], Rongchang Zhang [1], Zhiyun Ji [1] and Xuling Chen [1]

[1] School of Minerals Processing & Bioengineering, Central South University, Changsha 410083, China
[2] School of Metallurgy and Environment, Central South University, Changsha 410083, China
* Correspondence: csuganmin@126.com (M.G.); csufanxiaohui@126.com (X.F.)

Abstract: Iron ore sintering is a simple and sustainable way to treat zinc-bearing secondary resources. In this paper, the reaction behavior of zinc was studied by combining thermodynamic calculation and simulation tests under sintering temperature and atmosphere. The evolution law of Zn-containing phases during the heating process was also revealed. The results showed that Zn-containing substances were mainly converted to ZnO when the temperature reached 700 °C in the pre-drying zone, and ZnO started to combine with Fe_2O_3 to form $ZnFe_2O_4$ when the temperature reached 800 °C in the combustion zone. $ZnFe_2O_4$ remained stable at 1300 °C, and did not change in the atmosphere with low CO concentration. In conventional sintering conditions, the removal rate of zinc was about 5 wt%, zinc was mainly converted to $ZnFe_2O_4$ and stuck in the sinter. Therefore, to meet the zinc amount of the blast furnace load, pretreatment of raw materials or ore matching to control zinc content is necessary.

Keywords: zinc; iron ore sintering; reactive behavior; phase evolution

Citation: Lv, W.; Gan, M.; Fan, X.; Sun, Z.; Zhang, R.; Ji, Z.; Chen, X. Reaction Behavior and Transformation Path of Zinc in the Heating-Up Zone during Sintering Process. *Sustainability* **2022**, *14*, 10147. https://doi.org/10.3390/su141610147

Academic Editor: Saeed Chehreh Chelgani

Received: 29 June 2022
Accepted: 3 August 2022
Published: 16 August 2022

1. Introduction

In recent years, some of the zinc-containing resources with high zinc content, such as iron concentrate, dust and sludge, have been separately processed to recover zinc, others were sent to the sintering process because the zinc content was not up to the recovering requirement; it was gradually discovered that iron ore sintering is a simple and sustainable way to treat zinc-bearing secondary resources [1–3]. On the other hand, with the rapid development of the iron and steel industry, the world's high-grade iron ore resources are gradually scarce. During the sintering process, low-quality iron ores and secondary resources containing zinc are inevitably added [4,5]. In this way, the iron resources were fully used to prepare the blast furnace burden, and part of the metallurgical solid waste was consumed to reduce the environmental damage at the same time [6–8]. Therefore, it is of great significance for efficient utilization of metallurgical solid waste and sustainable development of the iron and steel industry that zinc-iron resources are used in iron ore sintering.

However, using zinc-containing iron ore and solid waste as sintering materials will increase the zinc content of sintered ore. According to the survey, China's blast furnace (BF) ironmaking is mainly based on sintered ore, in which the proportion of sintered ore is up to more than 70%. Zinc in the raw material can form zinc ferrite under certain conditions and remain in the sinter [9,10]. In this case, it can cause a lot of problems to BF, for instance, the blast furnace gas flow distribution will be abnormal, the tuyere will be upturned, the refractory brick will be damaged, and the life of the blast furnace shortened. Accordingly, controlling the zinc content of the sinter is particularly important [11–15]. Previous studies have shown that the zinc in sintering raw materials was mainly ZnS in iron ore and ZnO or zinc ferrite in secondary resources, ZnS was oxidized to form zinc oxide and sulfate in sintering production, and a very strong reducing atmosphere was needed to reduce and

remove zinc when its content was high [16–19]. The main mineral phases in the sinter with ZnO added were magnetite, calcium ferrite (SFCA), silicate and zinc ferrite [20]. The calcifier can convert zinc ferrite to zinc oxide at about 900–1000 °C [21]. Although a general understanding of zinc changes in the sintering process was known, the reaction behavior and transformation of zinc under different temperatures and atmospheres in each stage of the sintering process were far from unambiguous disclosure.

Therefore, in order to better treat zinc-bearing resources by sintering, it is necessary to study the behavior of zinc during the sintering process, and iron ore resources to provide theoretical support for the use of zinc; this paper studies the reaction of Zn with the main sintering components such as Fe, Ca, Si, and the special phase transformation certificate of Zn under sintering temperature atmosphere, revealing the reaction behavior and migration mechanism of Zn during the sintering process.

2. Materials and Methods

2.1. Materials

The raw materials for the sintering cup test were obtained from a large iron plant in China, it is a mixture of iron ore, flux, return ore, and miscellaneous materials. The mixture is mainly composed of Fe_2O_3, FeO and SiO_2, with a small amount of MgO and Al_2O_3.

Depending on the source of the raw materials' purchase, hematite was the main iron-bearing material. Zn content was about 0.02 wt% (Table 1). The chemical extraction method was used for detecting the chemical phase of the zinc in the sintering raw materials. According to the solubility of different morphologic elements, chemical reagents with different dissolution or exchange strengths were used to dissolve samples in sequence from weak to strong. Thus, the element to be measured in the sample was selectively extracted into a specific solution; then, the content of the element in the solution was determined. Test standard and operation methods referred to the literature [22,23]. As seen in Table 2, the zinc in raw materials predominantly exists as $ZnS/ZnFe_2O_4$, with a content of 87.1 wt%. $ZnCO_3/ZnO$, $ZnSiO_3$ and $ZnSO_4$ were also detected, accounting for 6.5 wt%, 5.6 wt% and 0.8 wt%, respectively.

Table 1. Sinter mixture composition/wt%.

Chemical Composition	Fe_2O_3	FeO	CaO	SiO_2	MgO	Al_2O_3	C	H2O	Zn	Pb
Content	63.83	9.01	8.61	4.79	1.77	1.43	3.57	7.00	0.02	0.01

Table 2. Phase distribution characteristics of Zn in sintered raw materials/wt%.

Phase	Zn	$ZnO/ZnCO_3$	$ZnS/ZnFe_2O_4$	$ZnSiO_3$	$ZnSO_4$
Content	-	6.5	87.1	5.6	0.8

2.2. Selection Basis of Experimental Conditions: Temperature and Atmosphere

The reaction of zinc in the sintering process was studied at different stages in specific temperatures and atmospheres. The temperature and atmosphere conditions in each stage and flue gas were shown in Table 3 [24,25]. The sintering process has an oxidizing atmosphere overall, while there is a local reducing atmosphere around when the fuel is burning violently. The temperature of the material layer in the initial stage of combustion is about 700 °C, and the temperature in the middle and later stages of combustion can reach more than 1300 °C. The combustion of fuels produces gases, such as CO, CO_2, and SO_2, which move with the flue down through the wet material belt. The temperature of the wet zone is below 100 °C, the moisture content is high and the SO_2 in the gas can be absorbed by the material layer. As the sintered flue gas enters the flue duct, the O_2 content is about 8–15%, the CO_2 content is 8–12%, and there are some gases such as CO and SO_2 (the gas percentages in this paper are all volume ratios). This paper focuses on the reaction of zinc in the heating-up zone, that is, the preheating zone and the combustion zone.

Table 3. Temperature and atmosphere at each stage of the sintering process.

Stage	The Temperature/°C	Atmosphere			
		O_2/%	CO/%	CO_2/%	SO_2/ppm
Sinter Zone	<1200	21	0	0	0
Combustion Zone	700–1300	21→8	0→2.0	0→12	0→2000
Drying Pre-Heating	100–700	8–15	0.5–2.0	8–12	200–2000
Wet Strip	<100	8–15	0.5–2.0	8–12	0
Exhaust Column	100–150	8–15	0.5–2.0	8–12	200–2000

The high-purity gases used in the test include O_2, N_2, CO, CO_2, Ar, etc. The gas purity is higher than 99.99%, the SO_2 gas concentration is 5000 ppm, and the balance gas is high-purity Ar.

2.3. Experimental Device and Method

The experimental setup for studying the reaction behavior of Zn was shown in Figure 1. The reactor is a high-temperature resistant quartz tube (Φ40 × 500 mm). Before starting, gas was introduced into the tube, and the flow rate was controlled using a rotameter. After the flow rate stabilized, the quartz tube was placed in a vertical tube furnace. The furnace adopts a KSY intelligent temperature control system, and the temperature of the reaction zone was calibrated by a standard thermocouple. Before the experiment, the air was introduced into the quartz tube, and the flow rate was controlled using a rotameter.

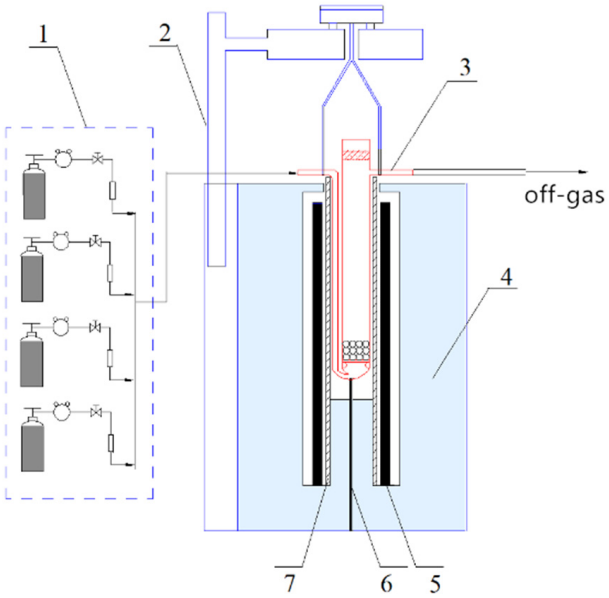

Figure 1. Schematic diagram of vertical tube furnace test system. (1) Air distributing device; (2) Stents; (3) High temperature resistant quartz reaction tube; (4) Fire-resistant and heat-retaining materials; (5) Silicon carbide; (6) Thermocouple; (7) Alundum tube.

The test steps are as follows: (1) Mix Fe_2O_3, CaO, SiO_2 and ZnO uniformly according to the ratio; (2) Add the proper amount of deionized water and mix well, use stainless steel grinding tool to make it into a pellet with a diameter of 5 mm and a height of about 5 mm, dried in an oven at 70 °C for 4 h; (3) The dried agglomerates are sent to the porous sieve plate at the bottom of the quartz tube along the wall of the quartz tube, and the gas required for the test is passed; (4) After the flow rate is stabilized, put the quartz tube in a shaft furnace at the target temperature for baking for a certain period of time and take it out, pass it through N_2 protection; (5) After cooling, take the sample out, put it in an agate mortar and grind it for use. When roasting in a reducing atmosphere, first pass the air in the N_2 evacuation system, put the quartz tube in the shaft furnace and wait for the temperature

to stabilize, then turn on CO_2, turn off N_2, and then pass CO; after the roasting, turn off CO, turn on N_2 Then turn off the CO_2 and take out the quartz tube for cooling; after the sample is cooled in the N_2 protective gas for a period of time, take it out and quickly put it in liquid nitrogen, then dry and grind.

The phase composition of the calcined product was detected using an X-ray diffractometer (Brook Advance D8, Billerica, MA, USA), with a conventional test scan step size of 0.02° and scan speed of $10°/min^{-1}$; refined scan step size of 0.01° and scan speed of $0.6°/min^{-1}$ [26,27]. The test results are imported into Jade 6.0 software for analysis.

When studying the possible reaction of lead and zinc in the sintering process, the standard Gibbs free energy of the reaction was used to judge whether the reaction can proceed spontaneously. In this paper, the standard Gibbs free energy of each substance was firstly identified, and then it was calculated according to the reaction equilibrium equation. All thermodynamic data were from Factsage7.2 (Thermfact/CRCT: Montreal, QC, Canada and GTT-Technologies: Aachen, Germany) and HSC6.0 thermodynamic software. Factsage 7.2, which can calculate, draw, edit units and multiphase pictures, was used to draw phase diagrams; they can analyze the mutual transformation of various phases, the formation of new phases and the disappearance of old phases in multiple systems under certain conditions. In this study, the Phase Diagram module was used to calculate the ternary Phase Diagram of the system under different atmospheres and temperatures. Taking the material composition as the coordinate axis, the oxidation and reduction atmosphere was set through the valence state of Fe element, and the isothermal section diagrams under different temperatures were made, respectively.

3. Experimental Results and Discussion

3.1. Reaction Thermodynamics of Zinc-Bearing Minerals during the Dry Pre-Heating Zone

The main Zn phase in the iron ore is ZnS. Due to the addition of some secondary materials, there are also some ZnO, $ZnFe_2O_4$, $ZnSO_4$, $ZnSiO_3$ and other substances. First, the possible reactions of ZnS, $ZnCO_3$ and $ZnSO_4$ in the pre-drying tropics are analyzed, as shown in Table 4.

Table 4. Conversion of ZnS, $ZnCO_3$, $ZnSO_4$ in raw materials ΔG_T^{Θ}-T.

Equations	ΔG_T^{Θ}-T (kJ/mol)	Remarks
$2ZnS + 3O_{2(g)} = 2ZnO + 2SO_{2(g)}$	$\Delta G_T^{\Theta} = 0.078T - 424.068$	Reaction 1
$ZnCO_3 = ZnO + CO_{2(g)}$	$\Delta G_T^{\Theta} = -0.142T + 11.929$	Reaction 2
$2ZnSO_4 = 2ZnO + 2SO_{2(g)} + O_{2(g)}$	$\Delta G_T^{\Theta} = -0.248T + 246.807$	Reaction 3

For a reaction involving gas, the partial pressure of the system has a significant effect on the reaction equilibrium [28].

$$a{\cdot}A(s) + b{\cdot}B(g) + c{\cdot}C(g) = d{\cdot}D(s) + e{\cdot}E(g) + f{\cdot}F(g) \quad (1)$$

Taking reaction (1) as an example, the reaction equilibrium constant can be expressed as:

$$K^{\Theta} = \frac{{P_{E(g)}}^{e} \times {P_{F(g)}}^{f}}{{P_{B(g)}}^{b} \times {P_{C(g)}}^{c}} \quad (2)$$

In the equation, $P_{B(g)}, P_{C(g)}, P_{E(g)}, P_{F(g)}$ Represents equilibrium partial pressures of reactants and products in each gas phase respectively. In the actual sintering system, reaction/product gases with a certain concentration may exist in the gas phase at the same time. Under specific gas phase partial pressures of the actual system, the reaction Gibbs free energy ΔG_T modified formula is:

$$\Delta G_T = \Delta G_T^{\Theta} + RT\ln\frac{{P_{E(g)}}^{e} \times {P_{F(g)}}^{f}}{{P_{B(g)}}^{b} \times {P_{C(g)}}^{c}} \quad (3)$$

Substitute the upper and lower limits of the actual gas concentration (CO_2, O_2, SO_2, etc.) of the dry pre-tropical zone shown in Table 3, respectively, to obtain the $\Delta G_T - T$ relationship of ZnS, $ZnCO_3$, $ZnSO_4$ conversion under the sintered dry pre-tropical zone system as shown in Figure 2. From the calculation results, it was clear that ZnS was very easy to convert into ZnO, and $ZnSO_4$ was also easy to decompose into ZnO at 10 °C under the condition of the sintering atmosphere. $ZnCO_3$ began to decompose and transform to ZnO at about 700 °C. The higher temperature was to the benefit of ZnO generating.

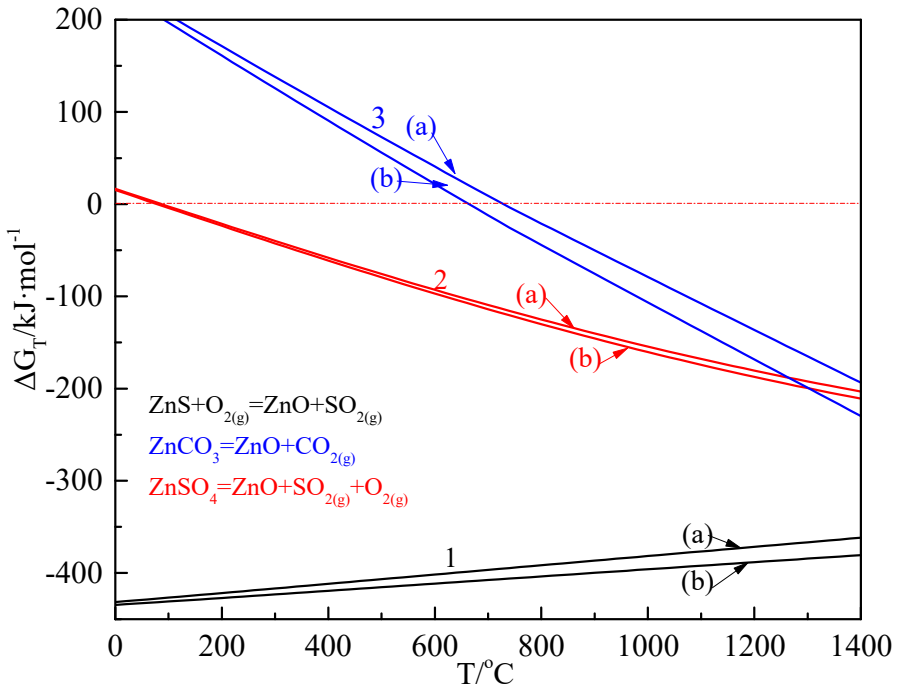

Figure 2. $\Delta G_T - T$ map of ZnS, $ZnCO_3$ and $ZnSO_4$ conversion. Reaction 1: (a) SO_2 = 0.2%, O_2 = 8%, (b) SO_2 = 0.02%, O_2 = 15%; Reaction 2: (a) CO_2 = 14%, (b) CO_2 = 8%; Reaction 3: (a) SO_2 = 0.2%, O_2 = 15%, (b) SO_2 = 0.02%, O_2 = 8%.

3.2. Conversion Behavior of Zn in the Combustion Zone

According to the analysis of Section 2.1, in the dry pre-heating zone, ZnS, $ZnCO_3$, and $ZnSO_4$ in the sintered raw materials are finally converted into ZnO, while $ZnFe_2O_4$, ZnO, and $ZnSiO_3$ may undergo a reduction reaction at a higher temperature and CO concentrations. First, the possible reduction reactions of $ZnFe_2O_4$, ZnO, $ZnSiO_3$ are shown in Table 5. Considering that in the actual reaction system, the presence of CO, CO_2, and Zn vapor has a significant effect on the reaction balance. Combining the range of CO concentration in the combustion zone shown in Table 3, draw the actual system ΔG_T-$RTlnP_{Zn(g)}$ diagram, as shown in Figure 3. The higher the temperature, the easier the reduction reaction will take place. At the same temperature, the higher the CO concentration, the easier the ZnO, $ZnFe_2O_4$, and $ZnSiO_3$ will be reduced to Zn(g), but under the sintering temperature and atmosphere conditions, the temperature is only higher than 1240 °C, it is possible to reduce to Zn(g), and the conditions for generating Zn(g) are harsh; under the same CO-CO_2 concentration, the reduction of the three compounds is relatively similar.

Table 5. Reduction of Zn-containing substances $\Delta G_T^{\ominus}$-T.

Equations	$\Delta G_T^{\ominus}$-T (kJ/mol)	Remarks
$ZnO + CO_{(g)} = CO_{2(g)} + Zn_{(g)}$	$\Delta G_T^{\ominus} = -0.021T + 67.493$	Reaction 4
$ZnFe_2O_4 + 2CO_{(g)} = 2CO_{2(g)} + 2FeO + Zn_{(g)}$	$\Delta G_T^{\ominus} = -0.040T + 71.638$	Reaction 5
$ZnSiO_3 + CO_{(g)} = Zn_{(g)} + CO_{2(g)} + SiO_2$	$\Delta G_T^{\ominus} = -0.029T + 74.758$	Reaction 6

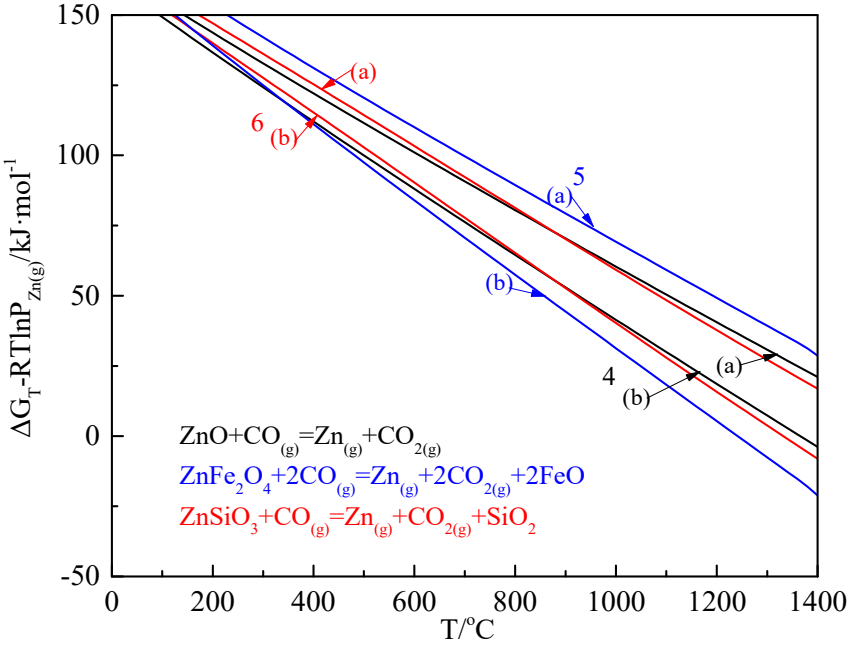

Figure 3. ΔG_T-$RTlnP_{Zn(g)}$ diagram of the reduction reaction of $ZnFe_2O_4$, ZnO and $ZnSiO_3$. Reaction 4: (a) CO_2 = 14%, CO = 0.5%, (b) CO_2 = 8%, CO = 2%; Reaction 5: (a) CO_2 = 14%, CO = 0.5%, (b) CO_2 = 8%, CO = 2%; Reaction 6: (a) CO_2 = 14%, CO = 0.5%, (b) CO_2 = 8%, CO = 2%.

To sum up, ZnS, $ZnCO_3$, $ZnSO_4$ can be converted to ZnO under the condition of a dry pre-tropical oxidizing atmosphere at a temperature of 100–700 °C; ZnO, $ZnFe_2O_4$, and $ZnSiO_3$ in the combustion zone may be reduced to elemental in the presence of CO and high-temperature Zn(g), but requires high temperature and high CO concentration. Figure 4 shows the chemical bitmap of the Zn-C-O system at different temperatures. The shaded part shows the sintering combustion zone atmosphere conditions; it can be seen that under the combustion zone conditions, Zn mainly exists in the form of ZnO, and it is more difficult to form elemental Zn(g).

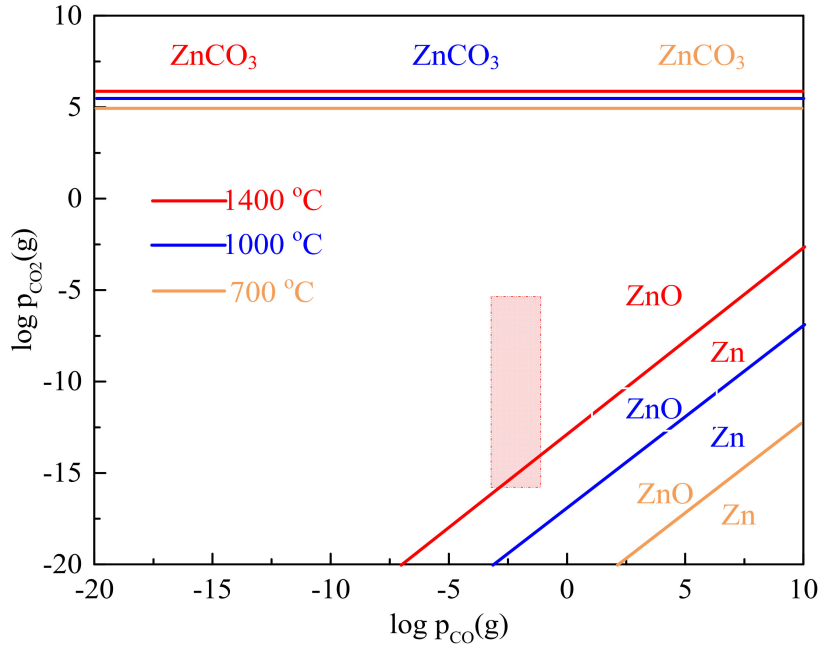

Figure 4. Chemical bit map of Zn-C-O system at different temperatures.

3.3. Reaction Behavior of ZnO with Fe, Ca and Si Oxides in Raw Materials

The Zn-containing phase entering the combustion zone is mainly ZnO. Therefore, with ZnO, Fe_2O_3, CaO, SiO_2 mixed samples as the object, the reaction behaviors of ZnO with Fe, Ca, Si under different temperatures, basicity, and atmosphere were studied. The standard ratio is: Fe_2O_3 + CaO + SiO_2 total iron content (TFe%) 52 wt%, CaO/SiO_2 mass ratio is 1.8, in order to better reflect the reaction between Zn and iron-containing materials, the quality of ZnO blended in of total Fe_2O_3 + 10 wt% of the mass of CaO + SiO_2.

3.3.1. Influence of Temperature

The roasting products under different temperatures were analyzed by XRD, the results were shown in Figure 5; it is understood that when the calcination temperature increased to 800 °C, $ZnFe_2O_4$ began to generate. With the increase of temperature, the amount of $ZnFe_2O_4$ gradually increased. When the temperature was 900 °C, calcium ferrite began to form in the product, so the combination of Zn, Ca and iron oxide was mainly generated in the temperature range of 900–1100 °C, and $ZnFe_2O_4$ and $CaFe_2O_4$ were mainly generated in the calcined product. When the temperature rose to 1300 °C, the phases of Fe_2O_3 and $CaFe_2O_4$ disappeared in the XRD pattern, but the phase of $ZnFe_2O_4$ still existed, indicating that $ZnFe_2O_4$ was more stable at 1300 °C.

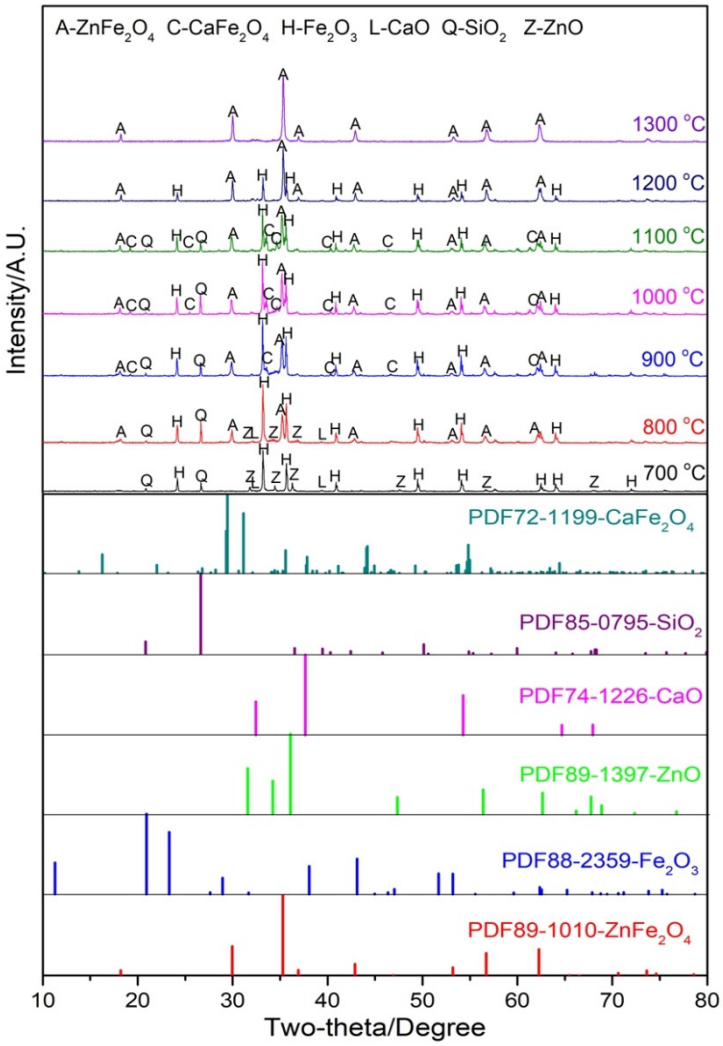

Figure 5. XRD patterns of calcined products of Fe_2O_3-CaO-SiO_2-ZnO at different temperatures (air atmosphere).

Figure 6 shows the phase diagram of the system at 1000 °C and 1300 °C. Figure 6a shows that when the basicity is 1.8 at 1000 °C, the main phase of the product is the spinel phase ($ZnFe_2O_4$), calcium ferrite ($CaFe_2O_4$) and calcium silicate, and no liquid phase appears in the system. The calculated results are basically consistent with the XRD results (Figure 5). As the roasting time selected in the experiment is only 10 min, there is still some unreacted quartz phase (SiO_2) in the roasted products. In Figure 6b, when the calcination temperature reaches 1300 °C, only the Spinel phase ($ZnFe_2O_4$) and liquid phase in the corresponding phase diagram (Figure 5); this result is consistent with XRD analysis, and the only $ZnFe_2O_4$ exists in the calcined products because the silicate liquid phase is cooled to form the glass phase, and XRD cannot detect the corresponding diffraction peak.

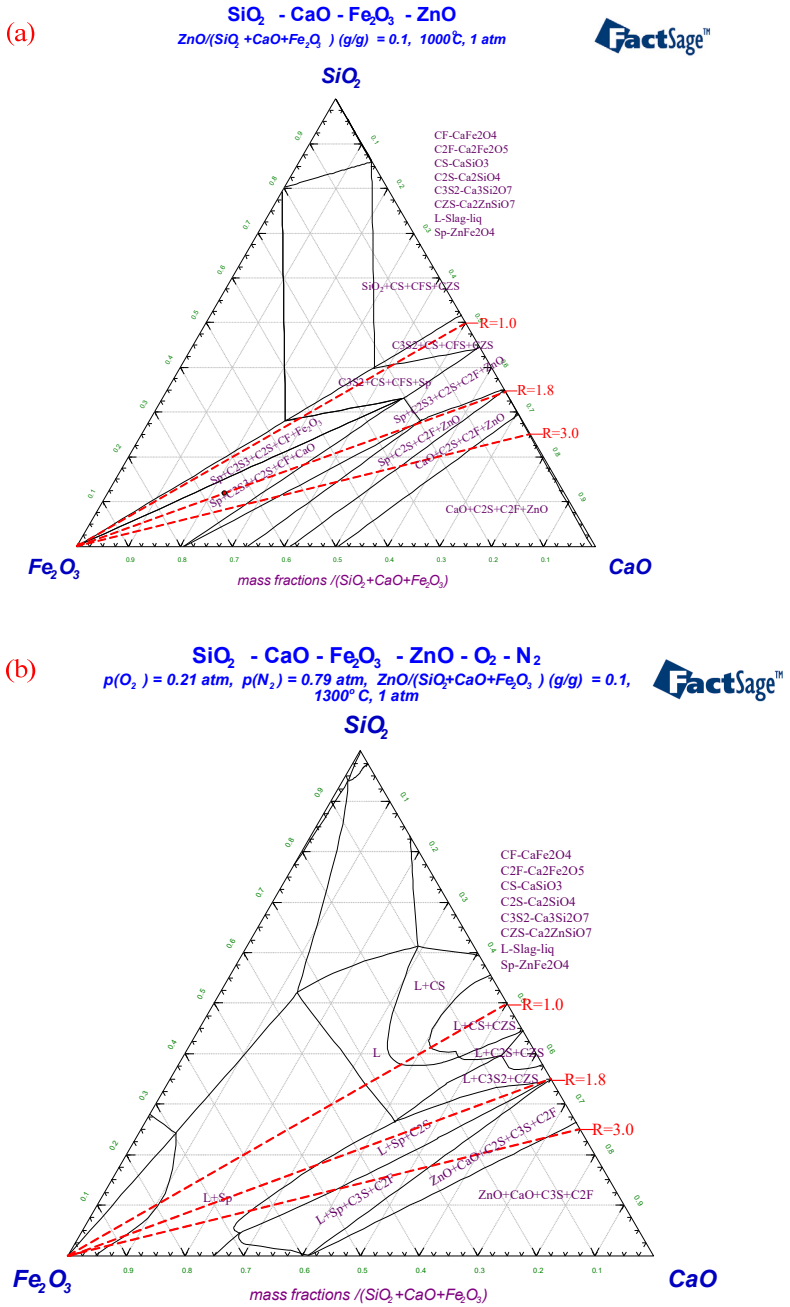

Figure 6. Phase diagram of Fe_2O_3-CaO-SiO_2-ZnO system in an oxidizing atmosphere. (**a**) 1000 °C isothermal section; (**b**) 1300 °C isothermal section.

3.3.2. The Effect of Basicity

The basicity (mass ratio of CaO/SiO_2, marked as R) of sintering raw materials has an important influence on the reaction in the system. Both CaO and ZnO can combine with Fe_2O_3, while SiO_2 can also react with ZnO. Figure 7 shows the phase composition of roasted products obtained from samples with different basicity roasted in the air. When CaO/SiO_2 is 1.2, $ZnFe_2O_4$ is generated instead of ZnO in the roasting product, indicating that ZnO has been completely combined with Fe_2O_3 and transformed into $ZnFe_2O_4$.With the increase of basicity, the peak value of $ZnFe_2O_4$ has no obvious change, while the peak strength of SiO_2 has obvious change; however, there is no other Si-containing phase in the XRD pattern, which is difficult to be detected by XRD due to the poor degree of silicate crystallization. With the increase of the basicity of raw materials, it can be seen that the diffraction peak of Fe_2O_3 in the roasted product is slightly weakened, while the diffraction peak of mono-calcium ferrite is gradually strengthened, indicating that the increase of basicity is conducive to the formation of calcium ferrite.

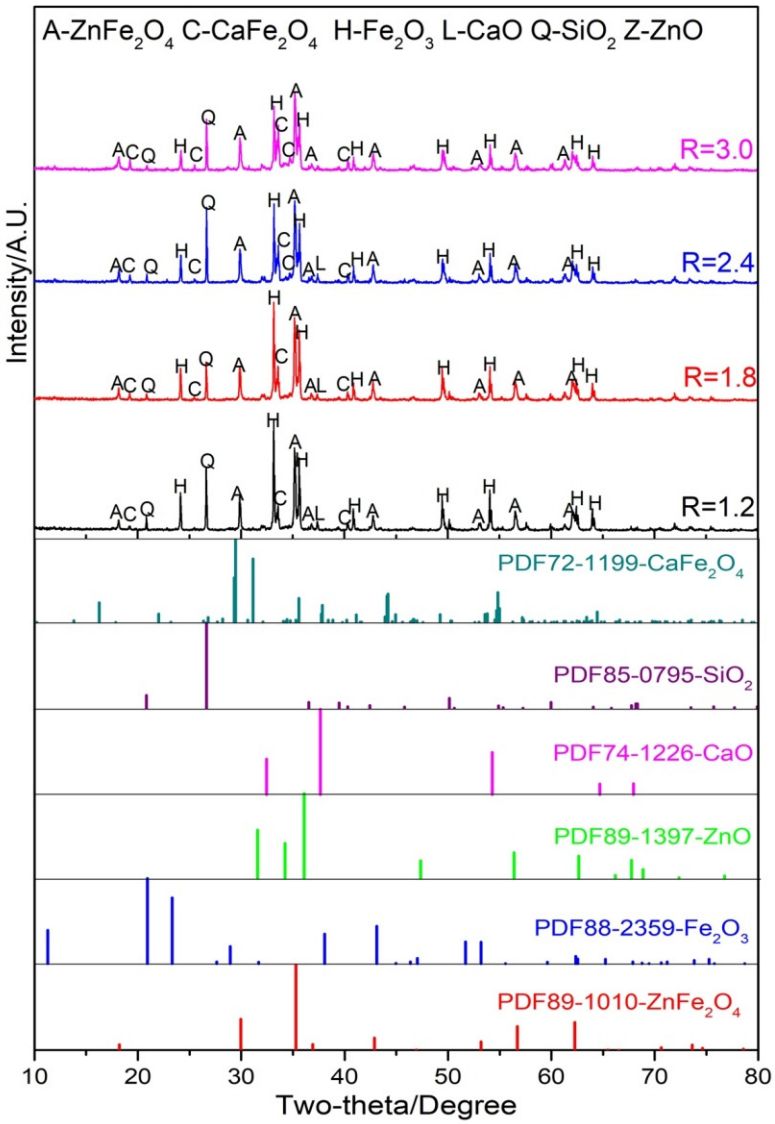

Figure 7. XRD patterns of calcined products of Fe_2O_3-CaO-SiO_2-ZnO with different CaO/SiO_2 (air atmosphere, 1000 °C).

As shown in Figure 7, when CaO/SiO_2 is 1.2, Ca_2ZnSiO_7 is generated in the system; when CaO/SiO_2 is more than 1.2, the Ca_2ZnSiO_7 phase in the system disappears, and the

Zn phase is transformed into ZnO and $ZnFe_2O_4$. The peak strength of Ca_2ZnSiO_7 could not be detected due to its low yield and poor crystallization. Therefore, when CaO/SiO_2 is 1.2, the Zn phase in the product is $ZnFe_2O_4$ and Ca_2ZnSiO_7; when CaO/SiO_2 is 1.8–3.0, the Zn phase in the product is still $ZnFe_2O_4$.

3.3.3. Influence of Reducing Atmosphere

In the actual sintering combustion zone, a certain concentration of CO exists. According to the calculation results in Section 2.2, CO concentration plays a decisive role in the reduction of substances containing zinc. Therefore, this section mainly studies the reaction behavior of ZnO with Fe, Ca and Si oxides in the weak reduction atmosphere of the actual sintering system. Figure 8 shows the phase composition of the products obtained by roasting samples with different CaO/SiO_2 ratios under an atmosphere of 1000 °C and $(CO/CO + CO_2)$ being 5%.

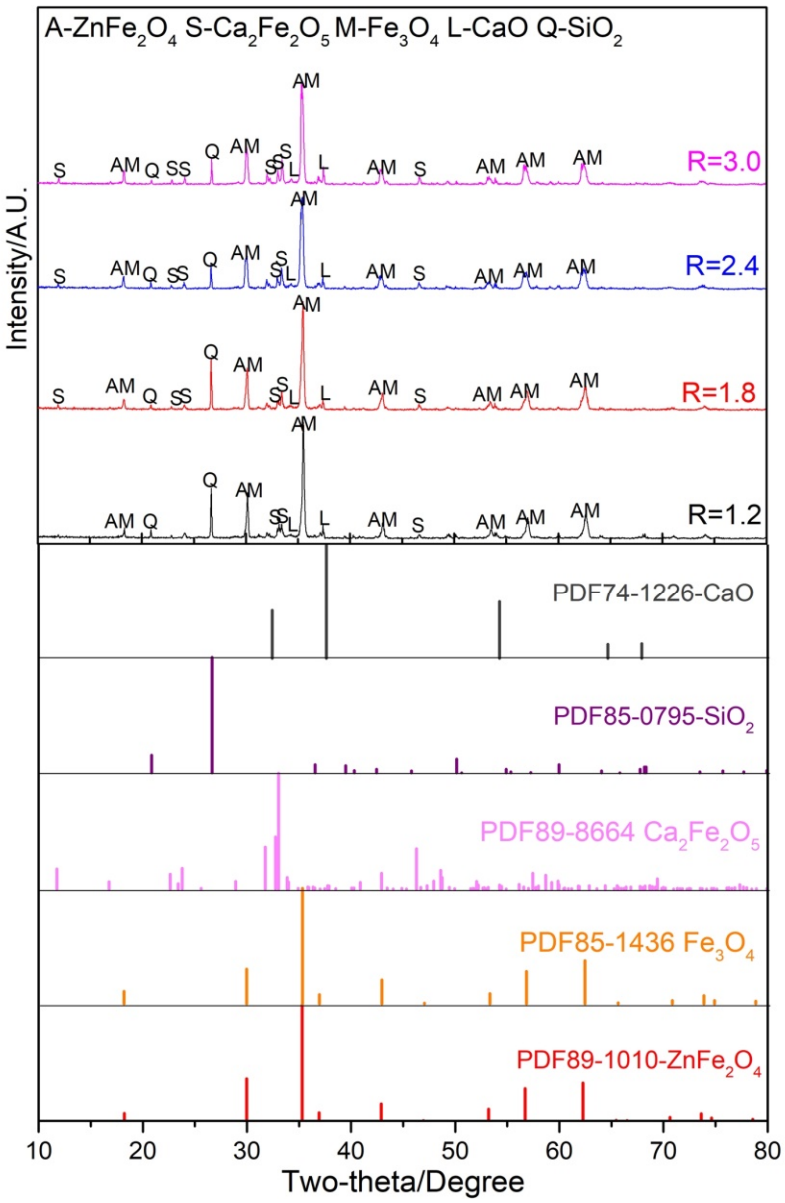

Figure 8. XRD patterns of calcined products of Fe_2O_3-CaO-SiO_2-ZnO with different CaO/SiO_2 (5% CO, 1000 °C).

The above indicates that Fe_2O_3 is reduced to Fe_3O_4, and $ZnFe_2O_4$ is generated in all calcined products, while CaO/SiO_2 has no obvious influence on the Phase of Zn in calcined products; however, with the increase of CaO/SiO_2, the peak value of SiO_2 gradually decreases, but there is no other phase containing Si. In the weak reduction atmosphere, the iron ore mainly combines with calcium to form dicalcium ferrite ($Ca_2Fe_2O_5$), and the diffraction peak strength of dicalcium ferrite gradually increases with the increase of basicity of raw materials.

Figure 9 shows the phase diagram at 1000 °C with 1 standard atmospheric pressure; it can be seen that similar to the air atmosphere, Ca_2ZnSiO_7 is formed in the system when CaO/SiO_2 is 1.2, and Ca_2ZnSiO_7 is converted into ZnO, $ZnFe_2O_4$ and calcium silicate compounds with the increase of CaO/SiO_2. Importantly, dicalcium ferrite is more stable than monocalcium ferrite in a weak reduction atmosphere. In the calculation results of the phase diagram, $Ca_2Fe_2O_5$ is one of the main iron-containing phases. When the basicity is higher than 1.8, the XRD results also show that the diffraction peak of the $Ca_2Fe_2O_5$ phase is significantly enhanced.

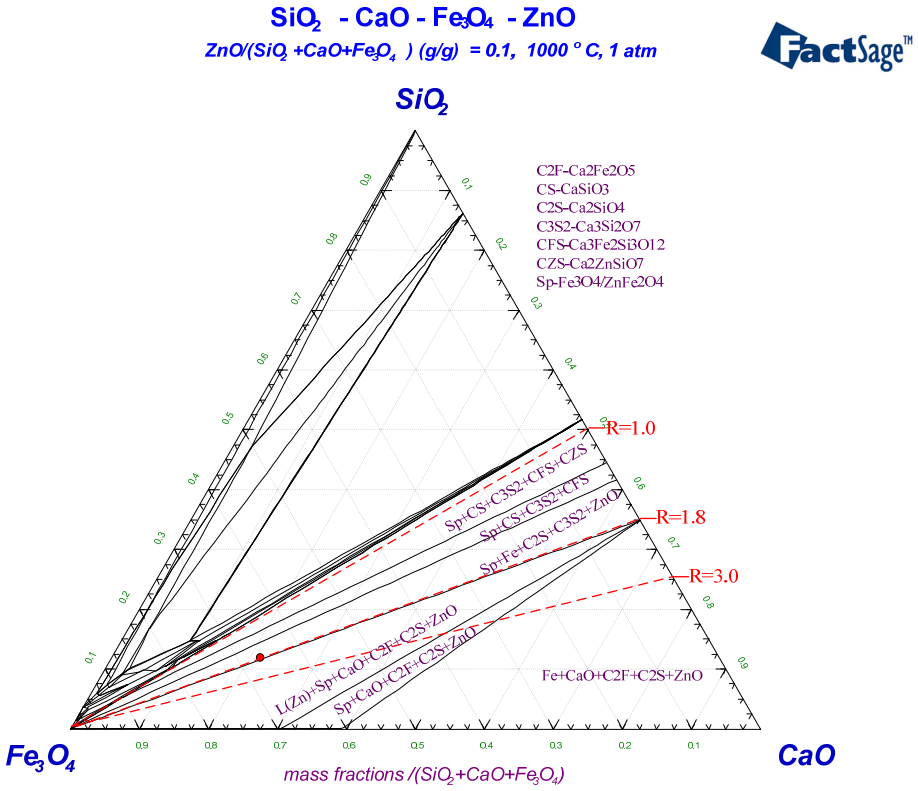

Figure 9. Weak reducing atmosphere Fe_3O_4-CaO-SiO_2-ZnO system phase diagram (1000 °C isothermal section).

3.4. Phase Transformation and Migration Behavior of Zn during Sintering

The sintering cup test was used to study the influence of carbon content on zinc removal in the conventional sintering process. The basicity of sintering raw materials was 1.8, the composition of the mixture was shown in Table 1, and the range of carbon content was 3.4–4.2 wt%. The test results were shown in Figure 10; it can be seen that under conventional sintering conditions, the higher the carbon content is, the higher the zinc removal rate will be; however, within the selected test range, the zinc removal rate is less than 10 wt%. When the carbon content (3.6 wt%) is suitable for the sintering production quality index, the zinc removal rate is only 5.3 wt%.

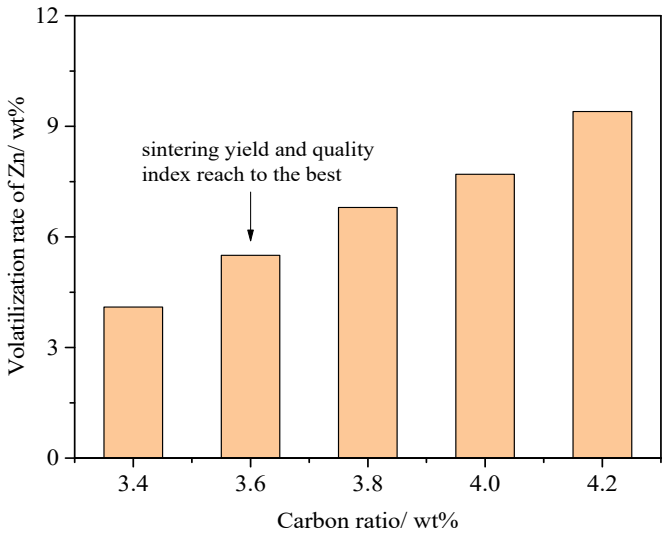

Figure 10. The effect of carbon content on the removal rate of Zn.

Table 6 shows the phase analysis results of zinc in sinter under conventional sintering conditions (carbon content 3.6 wt%); it can be seen that most of the Zn phases in sinter are converted to $ZnFe_2O_4$, and only a small amount exists in the form of ZnO or $ZnSiO_3$, which is basically consistent with the research results. According to the thermodynamic calculation and test results, combined with the temperature and atmospheric conditions of each sintering zone listed in Table 1, a schematic diagram of phase migration and transformation of Zn at each stage of the sintering process was obtained, as shown in Figure 11. $ZnSO_4$ and $ZnCO_3$ are decomposed to form ZnO. ZnO starts to combine with Fe_2O_3 to form $ZnFe_2O_4$ in the combustion zone at around 800 °C. Under conventional sintering conditions, the concentration of CO in the atmosphere is relatively low, and $ZnFe_2O_4$ is very stable and remains in the sinter.

Table 6. Phase distribution characteristics of Zn containing sinter/wt%.

ZnO	$ZnFe_2O_4$	$ZnSiO_3$	Others
2.7	95.7	1.6	Rarely

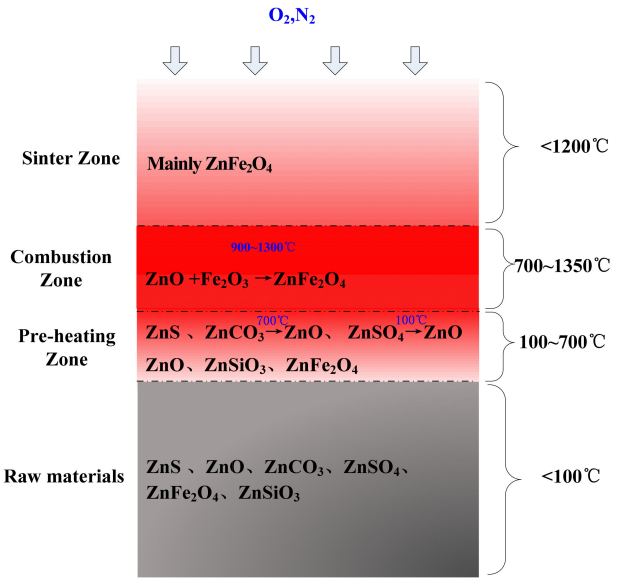

Figure 11. Schematic diagram of Zn phase migration and conversion.

4. Conclusions

In this paper, through thermodynamic calculation and simulated roasting test research, the reaction behavior of zinc in the sintering process was identified. Combining the temperature and atmospheric conditions of each zone in the sintering process, the conversion and migration laws of zinc were revealed:

(1) ZnS was easily oxidized to ZnO in pre-heating zone, meanwhile, $ZnSO_4$ was decomposed into ZnO at the beginning of pre-heating process. When the temperature was about 700 °C, $ZnCO_3$ also began to decompose and convert to ZnO. ZnO, $ZnSiO_3$, $ZnFe_2O_4$ in the raw materials remained no change under pre-heating temperature and atmosphere. Therefore, zinc existed mainly as ZnO, $ZnSiO_3$ and $ZnFe_2O_4$.

(2) When the temperature at the combustion zone was about 800 °C, ZnO started to combine with Fe_2O_3 to form $ZnFe_2O_4$, and the temperature increase was conducive to the reaction. When the temperature exceeded 1000 °C, ZnO would also react with Ca and Si to form a small amount of zinc-containing silicate phase. Under mild reducing conditions, $ZnFe_2O_4$ was very stable and remained in the solid phase of the sinter.

(3) Under conventional sintering conditions, the concentration of CO in the combustion zone was low; it was difficult to reduce the zinc oxide to elemental Zn by volatility. With the increase of carbon content, the corresponding zinc removal rate tended to increase. The removal rate of zinc was only up to 9.3% when carbon content increased from 3.4% to 4.2%; it was necessary to pretreat the raw materials to remove zinc or to control the zinc content of the raw materials through ore blending, or to increase the CO concentration in the feed layer by measures such as increasing the fuel ratio.

Author Contributions: Conceptualization, W.L., M.G. and X.F.; methodology, W.L., M.G. and Z.J.; validation, W.L., Z.J., M.G. and Z.S.; formal analysis, Z.S. and X.C.; investigation, W.L. and R.Z.; resources, M.G. and X.F.; data curation, W.L. and M.G.; writing—original draft preparation, W.L.; writing—review and editing, M.G. and X.F.; visualization, W.L.; supervision, X.F.; project administration, M.G. and X.F.; funding acquisition, M.G. All authors have read and agreed to the published version of the manuscript.

Funding: The research was financially supported by the National Natural Science Foundation of China (No. 51974371).

Institutional Review Board Statement: Not applicable.

Informed Consent Statement: Not applicable.

Data Availability Statement: All data for this study are available from the first or corresponding authors upon request.

Acknowledgments: We thank the anonymous reviewers for their valuable comments to improve the manuscript.

Conflicts of Interest: The authors declare no conflict of interest.

References

1. Barakat, M.A. The pyrometallurgical processing of galvanizing zinc ash and flue dust. *JOM* **2003**, *55*, 26–29. [CrossRef]
2. Yan, Y.; Zheng, G.S.; Zheng, S.L.; Hu, Z.B. Effects of depressant on recycling pyrite from tailings of lead-zinc ore. *Ind. Miner. Process.* **2015**, *1*, 14–16. (In Chinese)
3. Mehta, N.; Dino, G.; Passarella, I.; Ajmone-Marsan, F.; Rossetti, P.; De Luca, D. Assessment of the Possible Reuse of Extractive Waste Coming from Abandoned Mine Sites: Case Study in Gorno, Italy. *Sustainability* **2020**, *12*, 2471. [CrossRef]
4. Kaya, M.; Hussaini, S.; Kursunoglu, S. Critical review on secondary zinc resources and their recycling technologies. *Hydrometallurgy* **2020**, *195*, 105362. [CrossRef]
5. Han, J.; Liu, W.; Qin, W.; Jiao, F.; Wang, D.; Liang, C. Thermodynamic and kinetic studies for intensifying selective de-composition of zinc ferrite. *JOM* **2016**, *68*, 2543–2550. [CrossRef]
6. Zhang, Y.; Su, Z.J.; Han, B.L.; Jiang, T.; Anderson, C. A value-added multistage utilization process for the gradi-ent-recovery tin, iron and preparing composite phase change materials (C-PCMs) from tailings. *Sci. Rep.* **2019**, *9*, 14097.
7. Lanzerstorfer, C.; Bamberger-Strassmayr, B.; Pilz, K. Recycling of blast furnace dust in the iron ore sintering process: In-vestigation of coke breeze substitution and the influence on off-gas emissions. *ISIJ Int.* **2015**, *55*, 758–764. [CrossRef]

8. Wang, Y. Transformation Behavior and Removal Technology of Harmful Elements in Iron Bearing Dust during Sintering. Master's Thesis, Central South University, Changsha, China, 2018.
9. She, X.-F.; Wang, J.-S.; Wang, G.; Xue, Q.-G.; Zhang, X.-X. Removal Mechanism of Zn, Pb and Alkalis from Metallurgical Dusts in Direct Reduction Process. *J. Iron Steel Res. Int.* **2014**, *21*, 488–495. [CrossRef]
10. Kazinczy, B.; Kótai, L.; Gács, I.; Sajó, I.E.; Sreedhar, B.; Lázár, K. Study of the Preparation of Zinc(II) Ferrite and ZnO from Zinc- and Iron-Containing Industrial Wastes. *Ind. Eng. Chem. Res.* **2002**, *42*, 318–322. [CrossRef]
11. Zhang, Y.B.; Su, Z.J.; Zhou, Y.L.; Li, G.H.; Jiang, T. Reduction kinetics of SnO_2 and ZnO in the tin, zinc-bearing iron ore pellet under a 20%CO–80%CO_2 atmosphere. *Int. J. Miner. Process.* **2013**, *124*, 15–19. [CrossRef]
12. Lv, W.; Gan, M.; Fan, X.; Ji, Z.; Chen, X.; Yao, J.; Jiang, T. Recycling Utilization of Zinc-Bearing Metallurgical Dust by Reductive Sintering: Reaction Behavior of Zinc Oxide. *JOM* **2019**, *71*, 3173–3180. [CrossRef]
13. Zhao, L.; Sun, W.; Li, X.; Ye, Z.; Huang, J.; Zhang, G.; Cai, J. Assessment of particulate emissions from a sinter plant in steelmaking works in China. *Environ. Monit. Assess.* **2017**, *189*, 368. [CrossRef] [PubMed]
14. Chun, T.; Zhu, D. New Process of Pellets-Metallized Sintering Process (PMSP) to Treat Zinc-Bearing Dust from Iron and Steel Company. *Met. Mater. Trans. A* **2014**, *46*, 1–4. [CrossRef]
15. Mochizuki, Y.; Tsubouchi, N.; Akiyama, T. Reduction behavior and crushing strength of carbon-containing iron ore sinters prepared from tar recovered from coke oven gas. *Fuel Process. Technol.* **2015**, *138*, 704–713. [CrossRef]
16. Yabe, H.; Takamoto, Y. Reduction of CO_2 Emissions by Use of Pre-reduced Iron Ore as Sinter Raw Material. *ISIJ Int.* **2013**, *53*, 1625–1632. [CrossRef]
17. Donskov, E.G.; Lyalyuk, V.P.; Donskov, D.E. Carbon consumption in the blast furnace. *Steel Transl.* **2013**, *43*, 370–373. [CrossRef]
18. Yang, X.; Chu, M.; Shen, F.; Zhang, Z. Mechanism of zinc damaging to blast furnace tuyere refractory. *Acta Met. Sin.* **2009**, *22*, 454–460. [CrossRef]
19. Jeong, H.; Ra, K. Investigations of Metal Pollution in Road Dust of Steel Industrial Area and Application of Magnetic Separation. *Sustainability* **2022**, *14*, 919. [CrossRef]
20. Wang, X.; Wang, W.; Li, H.; Zhang, Q.; Yang, D.; Lin, G. Effect of ZnO on mineral phase and structure of sinter. *Iron Steel* **2021**, *56*, 7. (In Chinese)
21. Wang, C.; Guo, Y.; Yang, L.; Chen, F. Status and research progress of valuable metals recovery and utilization from Zinc bearing slag dust. *Metal Mine* **2019**, *3*, 9. (In Chinese)
22. Yin, M.; Li, J. *Petrology and Minerals*, 4th ed.; Geological Publishing House: Beijing, China, 2011.
23. He, X. Research on balance and removal behavior of harmful elements in iron ore sintering. Master's Thesis, Central South University, Changsha, China, 2016.
24. Fan, X.; Yu, Z.; Gan, M.; Chen, X.; Chen, Q.; Liu, S.; Huang, Y. Elimination Behaviors of NOx in the Sintering Process with Flue Gas Recirculation. *ISIJ Int.* **2015**, *55*, 2074–2081. [CrossRef]
25. Gan, M.; Fan, X.; Yu, Z.; Chen, X.; Lv, W.; Liu, S.; Huang, Y. Application of biomass fuel in iron ore sintering: Influencing mechanism and emission reduction. *Ironmak. Steelmak.* **2015**, *42*, 27–33. [CrossRef]
26. Zhang, Y.; Wang, J.; Cao, C.; Su, Z.; Chen, Y.; Lu, M. New understanding on the separation of tin from magnetite-type, tin-bearing tailings via mineral phase reconstruction processes—Science direct. *J. Mater. Res. Technol.* **2019**, *8*, 5790–5801. [CrossRef]
27. Zhang, Y.; Wang, J.; Su, Z.; Lu, M.; Jiang, T. Spinel $MnFe_2O_4$ nanoparticles (mfo-nps) for CO_2 cyclic decomposition pre-pared from ferromanganese ores. *Ceram. Int.* **2020**, *46*, 14206–14216. [CrossRef]
28. Su, Z.; Zhang, Y.; Han, B.; Liu, B.; Lu, M.; Peng, Z. Synthesis, characterization, and catalytic properties of nano-SnO by chemical vapor transport (cvt) process under CO-CO_2 atmosphere. *Mater. Design.* **2017**, *121*, 280–287. [CrossRef]